Am J Cancer Res 2023;13(6):2426-2438
www.ajcr.us /ISSN:2156-6976/ajcr0148774

*Original Article*

# Activation of the GPR35 on ILC2 drives immunosuppression to promote lung cancer progression

Jiawei Yue[1], Hui Guo[2], Peng Xu[1], Jinhong Ma[2], Yumin Wu[2,3]

*[1]Department of Orthopaedics, The Third Affiliated Hospital of Soochow University, Changzhou 213003, Jiangsu, China; [2]Department of Laboratory Medicine, The Third Affiliated Hospital of Soochow University, Changzhou 213003, Jiangsu, China; [3]Jiangsu Key Laboratory for Carbon-Based Functional Materials and Devices, Institute of Nano and Soft Materials (FUNSOM), College of Nano Science & Technology (CNST), Suzhou 215123, Jiangsu, China*

Received December 27, 2022; Accepted May 11, 2023; Epub June 15, 2023; Published June 30, 2023

**Abstract:** Lung cancer is the most common cancer type with poor prognosis. While G protein-coupled receptor 35 (GPR35) is a potent stimulator of tumor growth, group 2 innate lymphoid cells (ILC2) have shown dual effects in tumorigenesis. Intriguingly, inflammation induced GPR35 activation leads to an upregulation in the markers associated with ILC2. Here, we reported that GPR35 knockout mice exhibited a significantly reduced tumor growth and altered immune infiltration in tumors. Furthermore, activating GPR35 in different mouse models promoted tumor development by enhancing the production of IL-5 and IL-13, thereby facilitating the formation of the ILC2-MDSC axis. Moreover, we found that GPR35 was a poor prognostic factor in patients with lung adenocarcinoma. Together, our findings suggest the potential application of targeting GPR35 in cancer immunotherapy.

**Keywords:** G protein-coupled receptor 35 (GPR35), group 2 innate lymphoid cells (ILC2), immune infiltration, prognostic factor, immune therapies

## Introduction

Lung cancer is the most common cancer type and the leading cause of cancer-related death, with more than 2 million new cases and 1.7 million deaths globally each year. Approximately 85% of lung cancers are non-small cell lung cancer (NSCLC), of which more than 50% are adenocarcinomas [1]. Due to atypical symptoms, more than 70% of NSCLC patients present with advanced disease at diagnosis. Accumulating evidence has indicated that immunosuppression is the main cause of tumor-associated immune evasion. In the tumor microenvironment, cancer cells escape from immune surveillance by exploiting the tumor suppressing regulators [2].

As the most recently identified non-B and non-T cell family of immune cells, innate lymphoid cells (ILCs) lack antigen-specific receptors and can be classified into three groups according to the cytokine they secrete and the transcription factor they express, mirroring to some extent $CD4^+$ T helper subsets [3, 4]. While group 1 ILCs (ILC1s) secrete IFN-γ and express T-bet, group 2 ILCs (ILC2s) secrete IL-13 and IL-5, as well as express GATA3. In contrast, the tissue resident group 3 ILCs (ILC3s) secrete IL-22 and IL-17 and express RORγT [5]. Notably, several recent studies have highlighted the important contribution of ILC2 to various physiological and pathophysiological processes [6, 7]. Due to its unique occupational niche in mucosal tissue, ILC2s are one of the first-responder cells in the initiation of tumor-specific immune response. It has been reported that ILC2s exert their function mainly by producing cytokines IL-5 and IL-13 when activated by alarmins, thymic stromal lymphopoietin (TSLP), IL-25 or IL-33 [3]. Recently, several groups have reported the function of ILC2s in the tumor immune microenvironment (TIME). For example, Belz et al. found that IL-33 in combination with anti-PD-1 unleashed ILC2-mediated anti-melanoma immunity [8]. However, another study by Martijn et al. reported

that the activation of ILC2s promoted the lung tumor load via their capacity to suppress natural killer (NK) cell-mediated innate antitumor immunity [9]. Hence, the role of ILC2s in tumor development is controversial and requires further study.

G protein-coupled receptor 35 (GPR35) is an orphan G protein-coupled receptor that interacts with Na/K-ATPase [10]. GPR35 has been reported to be expressed in the intestinal epithelium, peripheral sensory neurons, and adipose, as well as in various myeloid cell types and cardiovascular tissue [11]. However, its function in tumor development is not fully understood. It has been reported that GPR35-deficient mice show reduced tumor development in mouse tumor model and in CAC model induced by sodium dextran sulfate (AOM-DSS) [10]. Kreider et al. reported that GPR35 promoted glycolysis, proliferation, and oncogenic signaling by engaging with the sodium-potassium pump [10]. A similar study showed that GPR35 expressed in macrophages is a potent tumor growth promoter by stimulating neoangiogenesis and tumor tissue remodeling [12]. Interestingly, one study has demonstrated that the activation of GPR35 upregulates the markers associated with ILC2s [13]. However, whether GPR35 is expressed as well as its function in ILC2 are still to be determined. Notably, kynurenic acid (KYNA), a product of the kynurenine pathway of tryptophan metabolism [14], has recently been reported as an agonist of GPR35 to exert immunosuppressive and anti-inflammatory effects [15-17].

In this study, we investigated the role of ILC2s and GPR35 in the development of lung adenocarcinoma (LUAD). We revealed that GPR35 regulated tumor growth in the murine LUAD model. Depletion of GPR35 profoundly reduced the tumor size in GPR35$^{-/-}$ mice, accompanied by the decreased number of ILC2s, while the activation of GPR35 resulted in the opposite effects. Therefore, our study has identified the tumor-promoting role of ILC2s and GPR35.

## Materials and methods

### *Reagents and antibodies*

IL-2 and IL-33 were purchased from R&D Systems, MN, USA; KYNA was from TOCRIS, MO, USA; Liberase was from Roche Diagnostics Corporation, IN, USA.

The following antibodies were purchased from Thermo Fisher Scientific, CA, USA: GPR35, FITC-lineage, Alexa Fluor 700-IFN-γ, while the following antibodies were purchased from Biolegend, CA, USA: CD3, CD28, APC-Cy7-CD45, PE-CD127, Percp-cy5.5-ST2, FITC-CD3, PE-Cy7-CD4, Percp-cy5.5-CD8, PE-Foxp3, APC-PD1, CD16/32, AF647-conjugated secondary antibody.

### *Mice*

GPR35$^{-/-}$ and Rag2$^{-/-}$ mice were generated in Shanghai Model Organisms Center, Inc. C57BL/6, GPR35$^{-/-}$ (C57BL/6-*Gpr35*$^{em1Smoc}$), and Rag2$^{-/-}$ (C57BL/6-*Rag2*$^{em2Smoc}$) mice were bred in our animal facility at Soochow University. Mice were housed in a pathogen-free barrier facility with a 12/12 h day/night cycle and free access to chow and water.

The experimental protocols were approved by the ethical committee of Soochow University (Suzhou, China), and all animal handlings were performed in accordance with the Declaration of Helsinki.

### *Cancer cell line*

The mouse LAUD LLC cells were cultured in DMEM medium (Sigma-Aldrich Co., St. Louis, MO, USA) supplemented with 10% FBS and 1% penicillin/streptomycin and maintained in a humidified atmosphere of 5% $CO_2$ at 37°C.

### *Mouse tumor models*

To initiate tumorigenesis, sex-matched 6-8 weeks old syngeneic C57BL/6, GPR35$^{-/-}$ or Rag2$^{-/-}$ mice were subcutaneously injected with LLC cells ($5 \times 10^5$) in the right flank, and the tumor growth was monitor. After tumor formation, the mice were randomized into different treatment groups. The GPR35 agonist KYNA was administered intraperitoneally every other day at a dose of 3 mg/kg. Tumor growth was measured every 2 or 3 days using a caliper. The tumor volume was calculated using the formula: $1/2 \times (\text{length} \times \text{width}^2)$. If the tumor reached 1500 $mm^3$ or became ulcerated, the mice were euthanized.

### *Recombinant IL-33 injection*

To administer rmIL-33, the mice were given intraperitoneal injections with 500 ng of carrier-free recombinant mouse IL-33 in sterile PBS

daily for three consecutive days. Then, the mice were sacrificed 24 h after the third injection, and the tumor samples were collected for further analysis.

*Single-cell isolation and flow cytometry*

Mouse tumor tissues were cut into small pieces, suspended in RPMI-1640 medium containing Liberase, and digested in a shaker at 37°C for 30 minutes. After centrifugation, the supernatants were passed through a 200 μm cell filter by centrifugation at 500×g for 5 minutes to obtain single-cell suspensions. These cells were first blocked with anti-mouse CD16/32 for 20 minutes at 4°C before staining with the following conjugated primary antibodies: FITC-lineage, Alexa Fluor 700-IFN-γ, APC-Cy7-CD45, PE-CD127, Percp-cy5.5-ST2, FITC-CD3, PE-Cy7-CD4, Percp-cy5.5-CD8, PE-Foxp3, APC-PD1.

To detect the expression of GPR35, primary antibody against GPR35 was used, followed by incubation with AF647-conjugated secondary antibody in the dark for 30 minutes at room temperature.

To detect intracellular cytokine production, single cell suspensions were first stimulated with a cell-stimulating cocktail (Thermo Fisher Scientific, CA, USA) for 6 h at 37°C. Then, the cells were stained for surface markers, or fixed, permeabilized, and stained for cytokine production using the Fixation and Permeabilization Buffer Kit (Thermo Fisher Scientific, CA, USA) according to the manufacturer's instructions. For Foxp3 staining, TM Foxp3/transcription factor staining buffer sets (eBioscience™, AUT) was used after surface marker staining. The labeled cells were quantified by the fluorescence-activated cell sorting (FACS) CantoII cell analyzer (BD Biosciences, CA, USA), and the FACS data were analyzed using Flowjo10 software (version 7.6.5; Tree Star, Ashland, OR, USA).

Mouse immune cells were defined as follows: ILC2s = live, $CD45^+$, $Lineage^-$ $CD127^+$, $ST2^+$ cells; T cells = live, $CD45^+$, $CD3^+$; $CD8^+$ T cells = live, $CD45^+$, $CD3^+$, $CD8^+$; $CD4^+$ T cells = live, $CD45^+$, $CD3^+$, $CD4^+$; regulatory T cells = live, $CD45^+$, $CD3^+$, $CD4^+$, $FoxP3^+$.

*Isolation of murine ILC2s and Pan T cells*

ILC2s were isolated from mouse splenocytes on a FACS Aria II system. Briefly, the murine splenic cell suspension was incubated with FITC-lineage (CD3ε, CD45R, Gr-1, CD11c, CD11b, Ter 119, NK1.1, TCR-αβ, and FCεRI), PE-CD127, as well as Percp-ST2, and then ILC2s were sorted by flow cytometry. Cells were stimulated with IL-2 (20 ng/ml) and IL-33 (10 ng/ml) for 72 h before use. Pan T cells were isolated by MACS Pan T cell isolation kit (Miltenyi Biotec, CA, USA). The sorted T cells were then cultured in standard culture medium at a density of $2 \times 10^5$ cells/well in 96-well plates (Costar) and stimulated with anti-CD3 (5 μg/ml) plus anti-CD28 (2 μg/ml) and IL-2 (20 ng/ml) for 72 h before use.

*Enzyme-linked immunosorbent assay (ELISA)*

The expression levels of IL-5 and IL-13 were measured by ELISA (Thermo Fisher Scientific, CA, USA) following the manufacturer's instructions. Each sample was examined in triplicate.

*Adoptive transfer*

To evaluate the effect of KYNA on tumor growth in $Rag2^{-/-}$ mice, KYNA in PBS was administered 7 days before cancer cell inoculation and was given every other day until 1 day before cell inoculation. On days 2, 4, and 6 post-tumor implantation, $1 \times 10^6$ pan T cells were intravenously injected into $Rag2^{-/-}$ mice. Control mice were injected with PBS. Tumor samples were collected at the indicated time points for further analysis.

*Gene correlation analysis in GEPIA and Kaplan-Meier plotter*

We used GEPIA (http://gepia.cancer-pku.cn/) and Kaplan-Meier plotter (http://kmplot.com/analysis/) [18] to investigate the expression of GPR35 and its association with the prognosis in LUAD. The patient samples were divided into two groups based on the expression level of GPR35, and the prognostic value of GPR35 was analyzed. The hazard ratio (HR) with 95% confidence intervals and log-rank *P*-value were also computed.

*Association of GPR35 with immune cell infiltration in LUAD*

First, the high-throughput RNA sequencing data [per Million base fragment (FPKM) format] and the corresponding clinicopathological information from the LUAD Project (KIRP) of the TCGA database were downloaded. Then, the single

sample GSEA method from the R package "GSVA" [19] was used to present the enrichment of infiltrating immune cells. Next, Spearman analysis was used to evaluate the relationship between GPR35 expression and immune cell infiltration, and the Wilcoxon rank sum test was used to compare the levels of immune cell infiltration in high- and low-GPR35 expression groups.

*Statistical analysis*

The experiments were independently repeated at least 3 times. The student t-test was used to compare groups, while two-tailed student t-test was used to compare unpaired data between groups using Prism software (GraphPad Software Inc.). The error bar represents the standard error of the mean. The degree of significance was indicated as: $*P < 0.05$, $**P < 0.01$, $***P < 0.001$.

## Results

*Germline deletion of GPR35 suppressed tumor growth*

Previous studies have demonstrated that GPR35 in macrophages promotes tumor growth in colon cancer [12]. To investigate the role of GPR35 in lung cancer, we used GPR35 knockout mice to determine the effect of GPR35 depletion on tumor growth in vivo. We observed that the tumors in the GPR35$^{-/-}$ group were significantly smaller than those in the WT group (**Figure 1A** and Supplementary Figure 1). In addition, the GPR35$^{-/-}$ group exhibited a significant reduction in the level of ILC2s in the tumor compared to the WT group, while no significant changes were observed in the tumor-draining lymph node (TDLN) (**Figure 1B**, **1C**), suggesting the involvement of ILC2 in GPR35-promoted tumor growth. We further examined the changes in the population of various immune cell types, including NK, CD103$^+$DC, CD11b macrophage, M1, M2, CD4$^+$ T cell, and CD8$^+$ T cells. Our results revealed that the percentages of NK cells (**Figure 1D**, **1E**) and CD103$^+$DC (**Figure 1F**, **1I**) were higher in the GPR35$^{-/-}$ group compared to the WT group, whereas no significant difference were observed in other cell populations (**Figure 1G**, **1H**, **1J** and **1K**). Together, these data indicated that GPR35 deficiency significantly inhibited the number of ILC2s but increased the population of NK and CD103$^+$DC cells in the tumor microenvironment.

*Activating GPR35 promoted tumor growth*

Previous ligand screening studies have identified several potential ligands of GPR35; among them, KYNA, a product of tryptophan catabolism, is the most studied one [20]. To confirm the effect of GPR35 on tumor growth observed in GPR35 knockout mouse, we used an alternative approach of activating GPR35 by administering KYNA to tumor-bearing mice via intraperitoneal injection. Consistent with the results above, the activation of GPR35 by KYNA promoted tumor growth (**Figure 2A** and Supplementary Figure 2) and elevated the level of ILC2s in tumor tissues, with no effect on TDLN (**Figure 2B**, **2C**). Moreover, we analyzed the effect of GPR35 activation on the proportions of NK, CD103$^+$DC, CD4$^+$ T cell, and CD8$^+$ T cells and observed an obvious reduction in the levels of CD103$^+$DC and CD8$^+$ T cells (**Figure 2D**, **2F**, **2H**, **2I**), but no significant change was found in NK level (**Figure 2E**, **2H**). Importantly, we also found that GPR35 activation caused the exhaustion of CD8$^+$ T cells with an elevated expression of PD1 (**Figure 2G**, **2J**), although no change was observed in the percentage in CD4$^+$ T cells, suggesting that GPR35 activation promoted CD4$^+$ T cells polarization towards Treg (**Figure 2G**, **2J**).

*Upregulation of GPR35 in IL-33-stimulated ILC2s*

To explore the expression of GPR35 in ILC2s before and after IL-33 stimulation, we intraperitoneally injected IL-33 or PBS into WT mice on days 1, 4, and 7 (**Figure 3A**) and collected the lung tissues on day 8. As shown in **Figure 3B** and **3C**, in contrast to the low level of GPR35 in ILC2s (Supplementary Figure 3A), the expression level of GPR35 as well as the population of GPR35$^+$ ILC2s were significantly elevated by IL-33 injection (**Figure 3D**). Meanwhile, we quantified the population of ILC2s in WT and GPR35$^{-/-}$ mice and found that the number of ILC2s in the bone marrow, spleen, lung, and gut was similar between WT and GPR35$^{-/-}$ mice (**Figure 3E**, **3F**).

*GPR35 engagement in ILC2-promoted tumor growth*

It has been known that GPR35 expression is not limited to ILC2s but is also found in other immune cells, such as T cells. Therefore, we evaluated the function of GPR35 in Rag2$^{-/-}$ mice

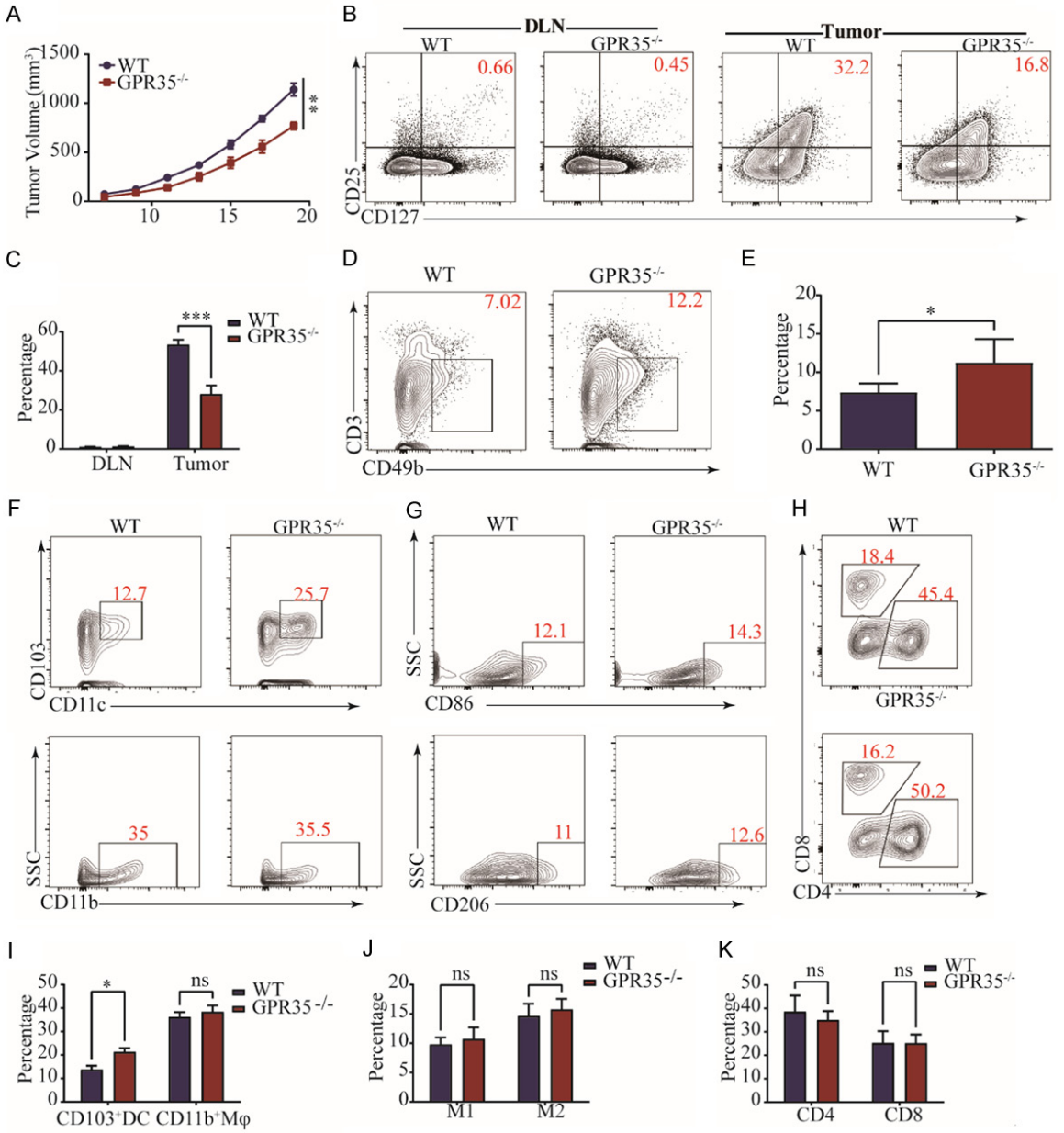


**Figure 1.** GPR35 deficiency inhibited tumor growth. (A) Tumors in GPR35$^{-/-}$ mice were strikingly smaller compared with tumors in WT mice. (B, C) The percentage of ILC2s in the tumors and in the TDLN of GPR35$^{-/-}$ and WT mice. The percentages of NK (D, E), CD103$^{+}$DC (F, I), CD11b macrophage (F, I), M1 (G, J), M2 (G, J), CD4$^{+}$ T cell (H, K), and CD8$^{+}$ T cell (H, K). All experiments were carried out in triplicate; data were presented as mean ± SD. $***P < 0.001$, $**P < 0.01$, $*P < 0.05$, ns, not significant.

where the adaptive branch of the immune system is defective but with normal ILC2s (**Figure 4A**). We found that GPR35 activation in Rag2$^{-/-}$ mice by KYNA treatment accelerated tumor development compared to non-treated mice (**Figure 4B** and Supplementary Figure 4). Meanwhile, an elevated percentage of ILC2s was found in the tumor tissues of the KYNA-treated group compared to the non-treated group (**Figure 4C**, **4D**). We also observed that the expression of GPR35 in the ILC2s of KYNA-treated mice was downregulated (Supplementary Figure 3B), which was consistent with previous reports. As GPR35 is internalized to initiate downstream signaling pathways upon KYNA stimulation [16], we also

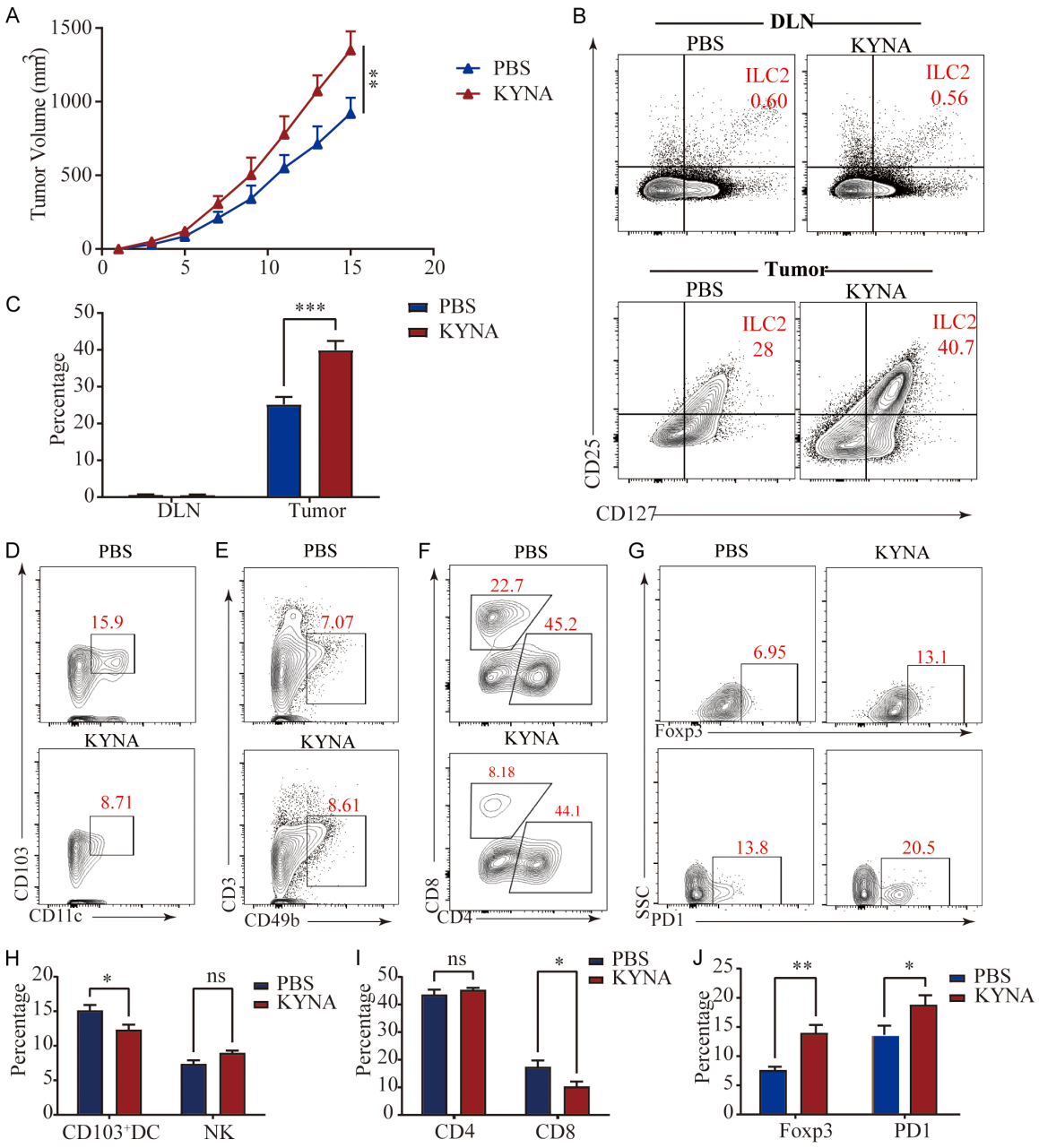


**Figure 2.** Activating GPR35 promoted tumor growth. (A) The activation of GPR35 by intraperitoneal administration of KYNA promoted tumor growth. (B, C) The percentage of ILC2s in the tumors and in the TDLN of the KYNA-treated and PBS-treated mice. The percentages of $CD103^+DC$ (D, H), NK (E, H), $CD4^+$ T cell (F, I), and $CD8^+$ T cell (F, I). The expression of Foxp3 in $CD4^+$ T cells (G, J) and the expression of PD1 in $CD8^+$ T cells (G, J). All experiments were performed in triplicate; data were presented as mean ± SD. $***P < 0.001$, $**P < 0.01$, $*P < 0.05$, ns, not significant.

found that the activation of GPR35 promoted the polarization of adoptive T cells towards Tregs (**Figure 4E**). Given that ILC2 can drive an immunosuppressive ILC2-MDSC axis via the secretion of IL-13, which could potentially contribute to tumor progression [21], we examined the population of MDSCs and obtained the similar results. Specifically, we observed a greater infiltration of MDSCs following GPR35 activation in $Rag2^{-/-}$ mice (**Figure 4F**, **4G**). Collectively, these results suggested the engagement of GPR35 in ILC2-promoted tumor growth and that the activation of GPR35 in ILC2 leads to the infiltration of MDSCs as well

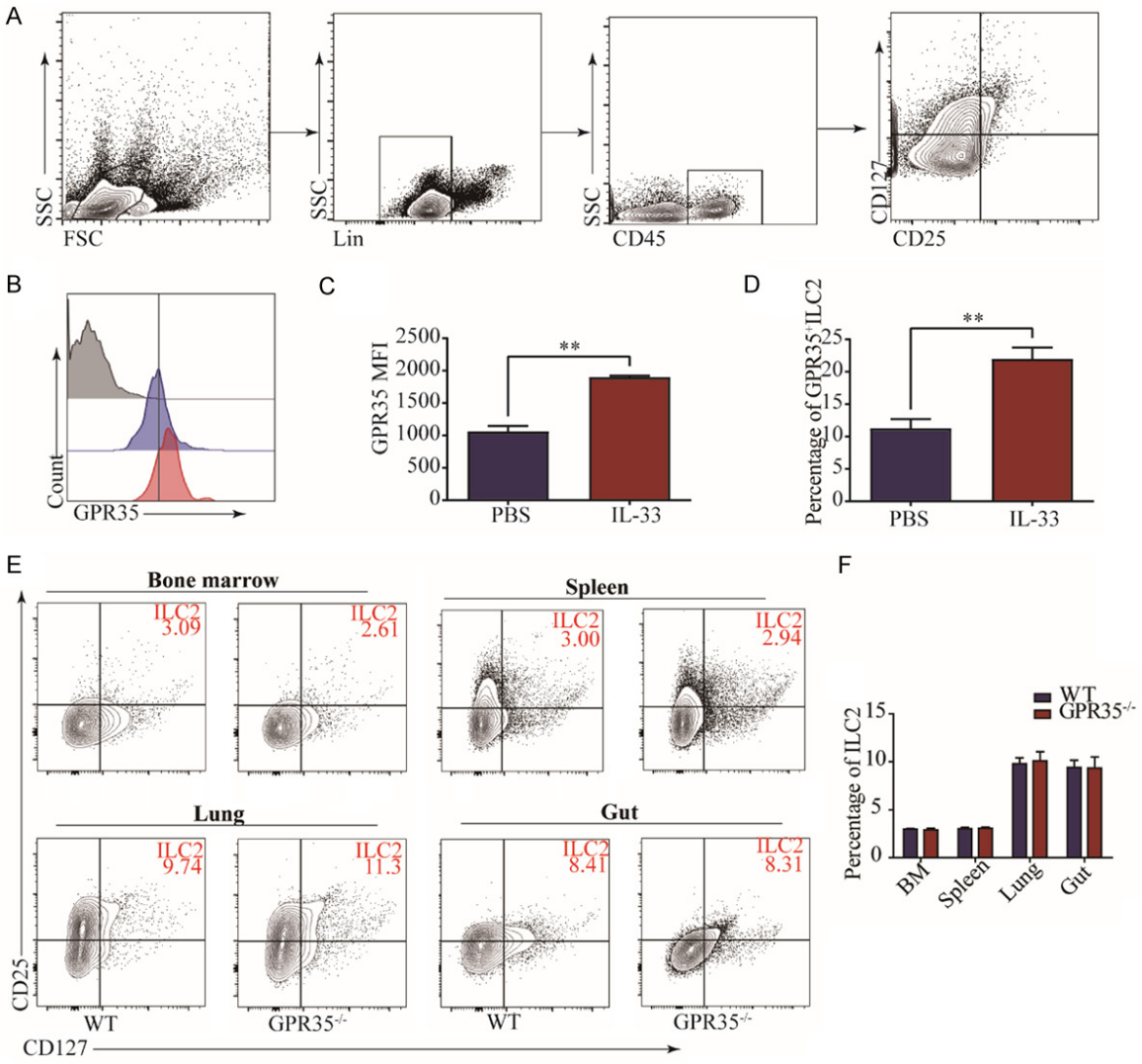


**Figure 3.** GPR35 deficiency had no effect on the development of ILC2s and an elevated GPR35 expression in IL-33-stimuated ILC2s. A. Gating strategy for ILC2s. B, C. The expression of GPR35 on ILC2s. D. The percentage of GPR35$^{+}$ ILC2s. E, F. The percentage of ILC2s in bone marrow, spleen, lung, and gut. All experiments were carried out in triplicate; data were presented as mean ± SD. $^{**}P < 0.01$, $^{*}P < 0.05$.

as promotes the polarization of adoptive T cells towards Tregs.

*Deficiency of GPR35 suppressed the production of IL-5 and IL-13 by ILC2s*

To evaluate the impact of GPR35 activation on cytokine secretion by ILC2s, we assessed the levels of IL-5 and IL-13 in ILC2s isolated from both WT and GPR35$^{-/-}$ mice. We first treated the freshly isolated ILC2s by recombinant mouse rmIL-33 for 48 and 72 h and then measured the cytokine secretion by FACS. Our results indicated that the secretion of IL-5 and IL-13 by GPR35-deficient ILC2s was significantly lower than that produced by WT ILC2s (**Figure 5**). To validate this conclusion, we also measured the levels of IL-13 and IL-5 secreted by ILC2s in culture medium by ELISA. Consistent with the FACS results, the levels of IL-13 and IL-5 were significantly lower in GPR35$^{-/-}$ mouse-derived ILC2s than in WT mouse-derived ILC2s (Supplementary Figure 5).

*Correlations between immune cell infiltration and GPR35*

It has been known that the expression of GPR35 on the surface of human iNKT cells is associated with a decreased IL-4 expression

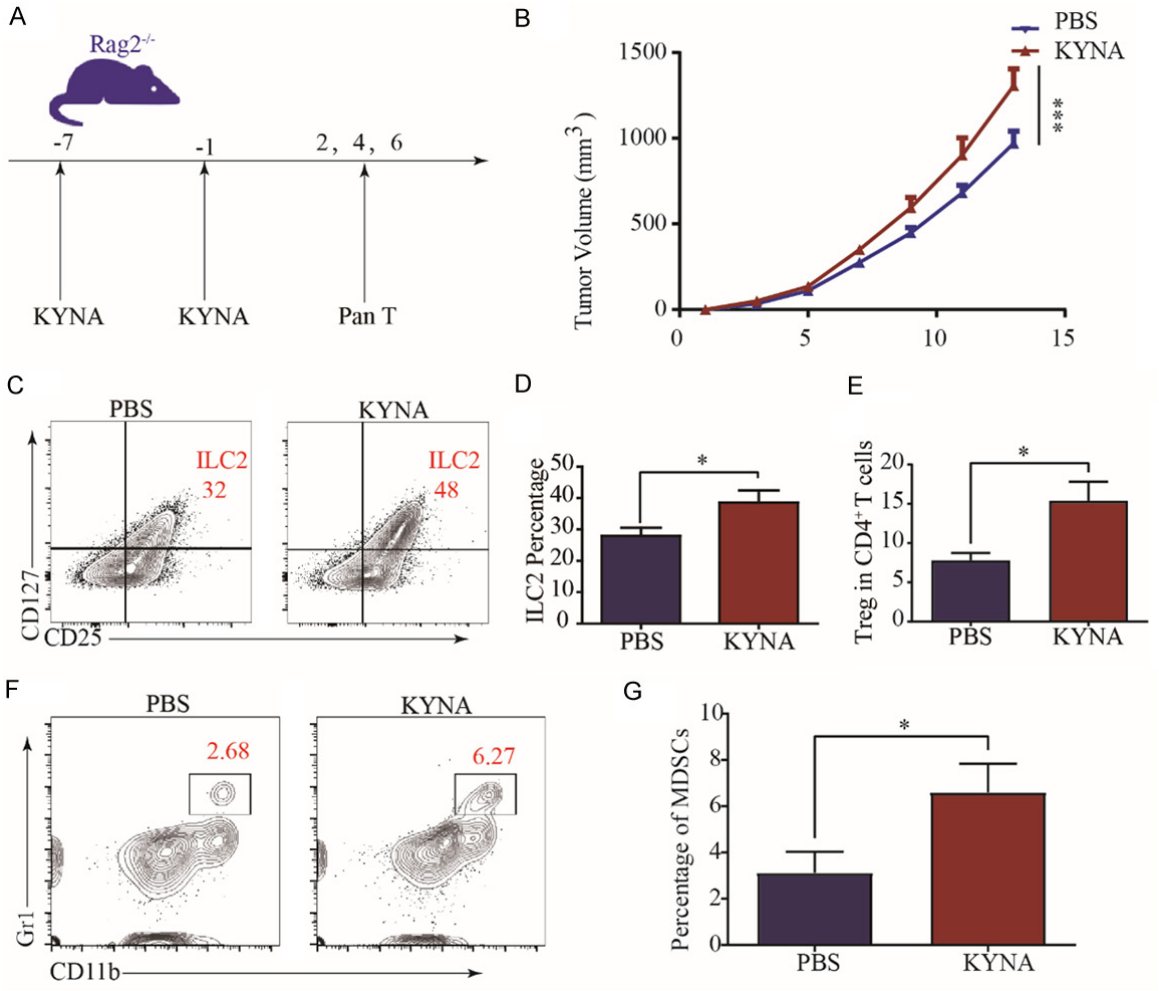


**Figure 4.** GPR35 engagement in ILC2-promoted tumor growth. A. The diagram of the model. B. Tumor growth curve. C, D. The percentage of ILC2s in the tumor. E. The percentage of Tregs in the tumor. F, G. The percentage of MDSCs in the tumor. All experiments were carried out in triplicate; data were presented as mean ± SD. ***$P < 0.001$, *$P < 0.05$.

[22]. Then, we explored the relationship of immune cell infiltration with GPR35 and observed a correlation between GPR35 expression and the infiltration of DCs, macrophages, mast cells, Th1 cells, and induced DC (iDC) (**Figure 6A**). In addition, we investigated the link between GPR35 and immunocompetence and found a negative correlation between GPR35 expression and several cancer-killing cells, including DCs (**Figure 6B**), macrophages (**Figure 6C**), mast cells (**Figure 6D**), Th1 cells (**Figure 6E**), and iDC (**Figure 6G**). Although we did not identify a significant correlation between GPR35 expression and Treg (**Figure 6H**) (P=0.07), our results suggested a positive association between them, consistent with the findings from the mice model. Nonetheless, we did not find any correlation between NK cells and GPR35 expression (**Figure 6F**).

*GPR35 was a poor prognostic factor in LUAD*

To evaluate the clinical relevance of GPR35, we analyzed its expression in LUAD tumor samples by using RNA sequencing data from the GEPIA database. The results showed that GPR35 expression was significantly higher in LUAD tumor samples than in normal tissues (Supplementary Figure 6A). To assess the prognostic significance of GPR35, we analyzed the overall survival (OS) and progression-free survival (PFS) of patients with LUAD by using data from TCGA database. Notably, we found that

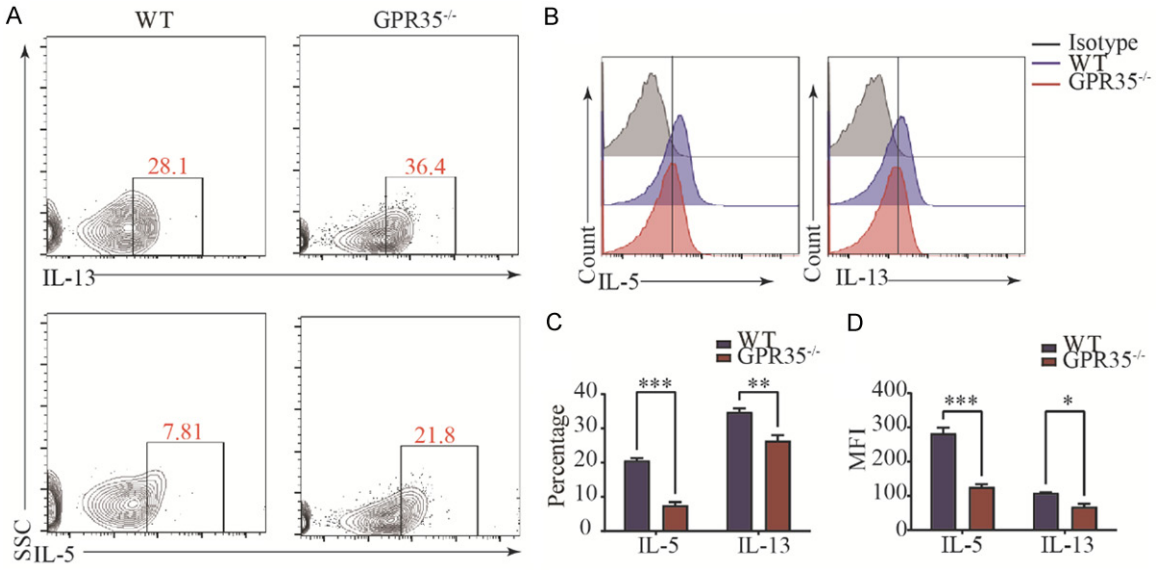


**Figure 5.** GPR35 deficiency in ILC2s suppressed the secretion of IL-5 and IL-13. A, C. The levels of IL-5 and IL-13 in WT and GPR35$^{-/-}$ mice. B, D. The MFI of IL-5 and IL-13. All experiments were carried out in triplicate; data were presented as mean ± SD. ***$P$ < 0.001, **$P$ < 0.01, *$P$ < 0.05.

lower GPR35 expression was associated with a better OS (Supplementary Figure 6B) and PFS (Supplementary Figure 6D) in patients with LUAD, while GPR35 expression had no prognostic value on squamous cell lung carcinoma (LUSC) (Supplementary Figure 6C).

## Discussion

ILC2s are increasingly recognized as a crucial regulator of Type-2 immune responses, exerting significant influence on downstream adaptive immunity in both healthy and disease states. However, the specific extrinsic and cell-intrinsic regulatory pathways that dictate ILC2 functions are still not fully understood. Recent studies have shown that ILC2s play a role in both anti-tumoral and pro-tumoral immunity in various mouse and human cancers. For example, Schuijs et al. have reported that mice treated with IL-33 have an amplified ILC2 immune response in the lung, which was induced by the secretion of IL-5, resulting in the activation of eosinophils. Subsequently, these eosinophils suppress the antitumor Th-1 immune response, thereby leading to an accelerated lung cancer metastasis and mortality [9]. Another study by Aftab et al. shows that the intratumoral mycobiome-driven secretion of IL-33 promotes tumor progression by recruiting and activating ILC2s and Th2 cells [23]. On the other hand, Lucarini et al. proposed that IL-33 could exhibit its cytotoxic effects by activating eosinophils to eliminate lung metastatic tumors and attenuate tumor progression [24]. Given these contradictory findings, it is critical to further investigate the specific role of ILC2s in tumor progression.

G protein-coupled receptors (GPCRs) are the largest family of cell surface receptors encoded by the human genome, with approximately 800 members. They regulate a vast array of cellular and physiological functions [25]. Among them, GPR35 has been shown to promote tumor progression. For example, GPR35 on macrophages has been found to facilitate tumor neovascularization and promote tumor growth [12]. Similarly, another study demonstrated that GPR35 could potently promote intestinal epithelial turnover and intestinal tumorigenesis [10].

In this study, we present evidence demonstrating the pro-tumor role of GPR35 in ILC2s in the context of LUAD. Our findings suggest that GPR35 promotes tumor progression, and its deficiency leads to an altered immune cell infiltration and an inhibited tumor growth. Furthermore, we observed that GPR35$^{-/-}$ mice had lower levels of ILC2s but higher levels of NK and CD103$^{+}$DC infiltration in the tumors compared to WT mice. Conversely, activating

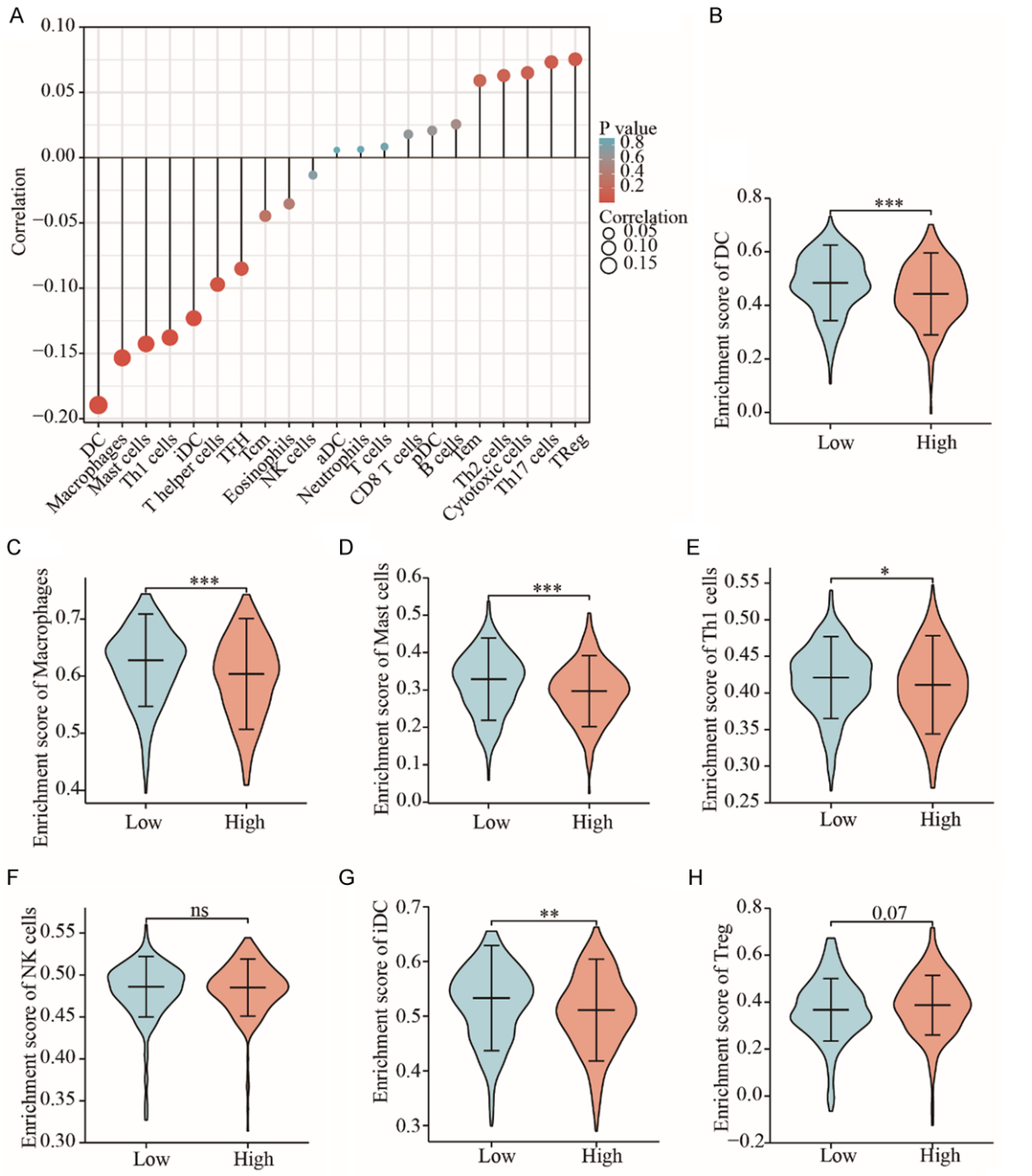


**Figure 6.** Correlations between immune cell infiltration and GPR35. Relationships between GPR35 expression and the infiltration of 21 immune cell types by Spearman's analysis. The most correlated immune cells (A), including DC (B), macrophages (C), mast cells (D), type 1 T helper cells (Th1) cells (E), and iDC (G) between the high- and low-GPR35 expression groups were shown. No significant correlation between GPR35 expression and NK cells (F) and Treg (H) was observed. All experiments were carried out in triplicate; data were presented as mean ± SD. ***$P$ < 0.001, **$P$ < 0.01, *$P$ < 0.05, ns, not significant.

GPR35 reduced the percentage of ILC2s, while increased the percentage of CD103$^+$DC infiltration in the tumors (**Figure 2**). It is well known that NK cells play a crucial role in innate immunity and possess potent antitumor abilities. They can not only directly kill cancer cells but also enhance the immune responses mediated by antibodies and T cells, making them a critical component of the immune surveillance against cancer [26]. As for CD103$^+$DCs, a previ-

ous study has demonstrated that $CD103^+$DCs are essential in antitumor function as $CD103^+$DCs are the only antigen-presenting cells (APCs) capable of transporting intact antigens to the lymph nodes and priming tumor-specific $CD8^+$ T cells [27].

Given that IL-5 promotes the development of antigen-specific $CD4^+CD25^+$ T regulatory cells (Tregs) [28] and that ILC2s are capable of producing IL-5, our findings suggest that the upregulation of ILC2s contributes to the polarization of $CD4^+$ T cells towards Tregs and the exhaustion of $CD8^+$ T cells. In this study, we observed elevated tumor infiltrating $PD1^+CD8^+$ T cells (**Figure 2J**) and $Foxp3^+CD4^+$ T cells (**Figure 2J**), indicating that the increased population of ILC2s promotes the accumulation of Tregs within the tumor microenvironment.

The functional versatility of ILC2s has been well established, as they can express a variety of receptors that mediate different biological functions [29, 30]. However, to our knowledge, no previous studies have investigated the expression of GPR35 on ILC2s, although Leandro et al. reported that the activation of GPR35 led to an altered expression of genes related to ILC2s and Treg function, suggesting a potential role of GPR35 in modulating inflammatory responses [17]. Here, to confirm the expression of GPR35 in ILC2s, we examined the expression of GPR35 in various cell types. Our results indicated that GPR35 was expressed on ILC2s, and that the stimulation of ILC2 by IL-33 led to an upregulation of GPR35. Interestingly, we also found that GPR35 deficiency did not affect the development of ILC2s (**Figure 3E**, **3F**). To investigate the role of GPR35-positive ILC2s in tumor growth, we utilized $Rag2^{-/-}$ mice to eliminate the interference of T cells when activating GPR35. In this model, we observed that the activation of GPR35 could still promote tumor growth in the absence of T and B cells (**Figure 4B**), accompanied by an increased ILC2s population within the tumor tissue (**Figure 4D**). Furthermore, we also observed that the activation of GPR35 led to an enhanced Tregs polarization after adoptive transfer with pan T cells (**Figure 4E**). Moreover, in consistent with previous findings that ILC2s can promote tumor progression by driving an immunosuppressive ILC2-MDSC axis through IL-13 [21], we found that the activation of GPR35 in $Rag2^{-/-}$ mice resulted in higher infiltration of MDSCs (**Figure 4F**, **4G**).

This study has also revealed that GPR35 activation impacts the invasion of ILC2s in tumor tissues. When we investigated the effect of GPR35 activation on the function of ILC2s, we found that GPR35 knockout attenuated the IL-33-induced production of IL-13 and IL-5 in ILC2s (**Figure 5B-D**). Previous studies have demonstrated that IL-5 is responsible for eosinophil activation, while IL-13 is associated with MDSCs that subsequently suppress immunity [9, 21], which is supported by our findings. Lastly, our bioinformatics analysis using the TCGA database also revealed that GPR35 was negatively correlated with DCs (**Figure 6B**), macrophages (**Figure 6C**), mast cells (**Figure 6D**), Th1 cells (**Figure 6E**), and induced DCs (**Figure 6G**). Although we did not find a significant correlation between GPR35 expression and Tregs, a weak positive correlation was observed (P=0.07) (**Figure 6H**). We also found that GPR35 was a poor prognostic factor in LUAD (Supplementary Figure 6).

In summary, this study was the first to investigate the expression of GPR35 in ILC2s and its impact on tumor immunity. Our findings suggest that GPR35 plays a crucial role in regulating ILC2 infiltration as well as the expression of IL-13 and IL-5, which in turn suppresses the function of MDSC in immune response. Hence, targeting ILC2s/GPR35 may be a promising strategy to modulate tumor immune response for the treatments of LUAD, which warrants further investigation on factors that trigger GPR35 activation in tumor tissues.

## Acknowledgements

This work was supported by grants from the National Natural Science Foundation of China (grant: 81801568), and the major project of Changzhou (grant: ZD202011).

## Disclosure of conflict of interest

None.

**Address correspondence to:** Yumin Wu and Jinhong Ma, Department of Laboratory Medicine, The Third Affiliated Hospital of Soochow University, Changzhou 213003, Jiangsu, China. E-mail: wuyumin1116@yeah.net (YMW); mjhczyy@126.com (JHM)

## References


[1] Siegel RL, Miller KD, Fuchs HE and Jemal A. Cancer statistics, 2022. CA Cancer J Clin 2022; 72: 7-33.

[2] Kleffel S, Posch C, Barthel SR, Mueller H, Schlapbach C, Guenova E, Elco CP, Lee N, Juneja VR, Zhan Q, Lian CG, Thomi R, Hoetzenecker W, Cozzio A, Dummer R, Mihm MC Jr, Flaherty KT, Frank MH, Murphy GF, Sharpe AH, Kupper TS and Schatton T. Melanoma cell-intrinsic PD-1 receptor functions promote tumor growth. Cell 2015; 162: 1242-1256.

[3] Klose CS and Artis D. Innate lymphoid cells as regulators of immunity, inflammation and tissue homeostasis. Nat Immunol 2016; 17: 765-774.

[4] Ercolano G, Wyss T, Salomé B, Romero P, Trabanelli S and Jandus C. Distinct and shared gene expression for human innate versus adaptive helper lymphoid cells. J Leukoc Biol 2020; 108: 723-737.

[5] Lim AI, Li Y, Lopez-Lastra S, Stadhouders R, Paul F, Casrouge A, Serafini N, Puel A, Bustamante J, Surace L, Masse-Ranson G, David E, Strick-Marchand H, Le Bourhis L, Cocchi R, Topazio D, Graziano P, Muscarella LA, Rogge L, Norel X, Sallenave JM, Allez M, Graf T, Hendriks RW, Casanova JL, Amit I, Yssel H and Di Santo JP. Systemic human ILC precursors provide a substrate for tissue ILC differentiation. Cell 2017; 168: 1086-1100, e10.

[6] Kato A. Group 2 innate lymphoid cells in airway diseases. Chest 2019; 156: 141-149.

[7] Bal SM, Bernink JH, Nagasawa M, Groot J, Shikhagaie MM, Golebski K, van Drunen CM, Lutter R, Jonkers RE, Hombrink P, Bruchard M, Villaudy J, Munneke JM, Fokkens W, Erjefält JS, Spits H and Ros XR. IL-1β, IL-4 and IL-12 control the fate of group 2 innate lymphoid cells in human airway inflammation in the lungs. Nat Immunol 2016; 17: 636-645.

[8] Jacquelot N, Seillet C, Wang M, Pizzolla A, Liao Y, Hediyeh-Zadeh S, Grisaru-Tal S, Louis C, Huang Q, Schreuder J, Souza-Fonseca-Guimaraes F, de Graaf CA, Thia K, Macdonald S, Camilleri M, Luong K, Zhang S, Chopin M, Molden-Hauer T, Nutt SL, Umansky V, Ciric B, Groom JR, Foster PS, Hansbro PM, McKenzie ANJ, Gray DHD, Behren A, Cebon J, Vivier E, Wicks IP, Trapani JA, Munitz A, Davis MJ, Shi W, Neeson PJ and Belz GT. Blockade of the co-inhibitory molecule PD-1 unleashes ILC2-dependent antitumor immunity in melanoma. Nat Immunol 2021; 22: 851-864.

[9] Schuijs MJ, Png S, Richard AC, Tsyben A, Hamm G, Stockis J, Garcia C, Pinaud S, Nicholls A, Ros XR, Su J, Eldridge MD, Riedel A, Serrao EM, Rodewald HR, Mack M, Shields JD, Cohen ES, McKenzie ANJ, Goodwin RJA, Brindle KM, Marioni JC and Halim TYF. ILC2-driven innate immune checkpoint mechanism antagonizes NK cell antimetastatic function in the lung. Nat Immunol 2020; 21: 998-1009.

[10] Schneditz G, Elias JE, Pagano E, Zaeem Cader M, Saveljeva S, Long K, Mukhopadhyay S, Arasteh M, Lawley TD, Dougan G, Bassett A, Karlsen TH, Kaser A and Kaneider NC. GPR35 promotes glycolysis, proliferation, and oncogenic signaling by engaging with the sodium potassium pump. Sci Signal 2019; 12: eaau9048.

[11] Quon T, Lin LC, Ganguly A, Tobin AB and Milligan G. Therapeutic opportunities and challenges in targeting the orphan G protein-coupled receptor GPR35. ACS Pharmacol Transl Sci 2020; 3: 801-812.

[12] Pagano E, Elias JE, Schneditz G, Saveljeva S, Holland LM, Borrelli F, Karlsen TH, Kaser A and Kaneider NC. Activation of the GPR35 pathway drives angiogenesis in the tumour microenvironment. Gut 2022; 71: 509-520.

[13] Agudelo LZ, Ferreira DMS, Cervenka I, Bryzgalova G, Dadvar S, Jannig PR, Pettersson-Klein AT, Lakshmikanth T, Sustarsic EG, Porsmyr-Palmertz M, Correia JC, Izadi M, Martínez-Redondo V, Ueland PM, Midttun Ø, Gerhart-Hines Z, Brodin P, Pereira T, Berggren PO and Ruas JL. Kynurenic acid and Gpr35 regulate adipose tissue energy homeostasis and inflammation. Cell Metab 2018; 27: 378-392, e5.

[14] Swartz KJ, During MJ, Freese A and Beal MF. Cerebral synthesis and release of kynurenic acid: an endogenous antagonist of excitatory amino acid receptors. J Neurosci 1990; 10: 2965-2973.

[15] Wirthgen E, Hoeflich A, Rebl A and Günther J. Kynurenic acid: the janus-faced role of an immunomodulatory tryptophan metabolite and its link to pathological conditions. Front Immunol 2017; 8: 1957.

[16] Wang J, Simonavicius N, Wu X, Swaminath G, Reagan J, Tian H and Ling L. Kynurenic acid as a ligand for orphan G protein-coupled receptor GPR35. J Biol Chem 2006; 281: 22021-22028.

[17] Agudelo LZ, Ferreira DMS, Cervenka I, Bryzgalova G, Dadvar S, Jannig PR, Pettersson-Klein AT, Lakshmikanth T, Sustarsic EG, Porsmyr-Palmertz M, Correia JC, Izadi M, Martínez-Redondo V, Ueland PM, Midttun Ø, Gerhart-Hines Z, Brodin P, Pereira T, Berggren PO and Ruas JL. Kynurenic acid and Gpr35 regulate adipose tissue energy homeostasis and inflammation. Cell Metab 2018; 27: 378-392, e5.

[18] Lanczky A, Nagy A, Bottai G, Munkacsy G, Szabo A, Santarpia L and Gyorffy B. miRpower: a web-tool to validate survival-associated miR-

NAs utilizing expression data from 2178 breast cancer patients. Breast Cancer Res Treat 2016; 160: 439-446.
[19] Hänzelmann S, Castelo R and Guinney J. GSVA: gene set variation analysis for microarray and RNA-seq data. BMC Bioinformatics 2013; 14: 7.
[20] Deng H, Hu H and Fang Y. Multiple tyrosine metabolites are GPR35 agonists. Sci Rep 2012; 2: 373.
[21] Trabanelli S, Chevalier MF, Martinez-Usatorre A, Gomez-Cadena A, Salomé B, Lecciso M, Salvestrini V, Verdeil G, Racle J, Papayannidis C, Morita H, Pizzitola I, Grandclément C, Bohner P, Bruni E, Girotra M, Pallavi R, Falvo P, Leibundgut EO, Baerlocher GM, Carlo-Stella C, Taurino D, Santoro A, Spinelli O, Rambaldi A, Giarin E, Basso G, Tresoldi C, Ciceri F, Gfeller D, Akdis CA, Mazzarella L, Minucci S, Pelicci PG, Marcenaro E, McKenzie ANJ, Vanhecke D, Coukos G, Mavilio D, Curti A, Derré L and Jandus C. Tumour-derived PGD2 and NKp30-B7H6 engagement drives an immunosuppressive ILC2-MDSC axis. Nat Commun 2017; 8: 593.
[22] Fallarini S, Magliulo L, Paoletti T, de Lalla C and Lombardi G. Expression of functional GPR35 in human iNKT cells. Biochem Biophys Res Commun 2010; 398: 420-425.
[23] Alam A, Levanduski E, Denz P, Villavicencio HS, Bhatta M, Alhorebi L, Zhang Y, Gomez EC, Morreale B, Senchanthisai S, Li J, Turowski SG, Sexton S, Sait SJ, Singh PK, Wang J, Maitra A, Kalinski P, DePinho RA, Wang H, Liao W, Abrams SI, Segal BH and Dey P. Fungal mycobiome drives IL-33 secretion and type 2 immunity in pancreatic cancer. Cancer Cell 2022; 40: 153-167, e11.
[24] Lucarini V, Zicchedda G, Macchia I, La Sorsa V, Peschiaroli F, Buccione C, Sistigu A, Sanchez M, Andreone S, D'Urso MT, Spada M, Macchia D, Afferni C, Mattei F and Schiavoni G. IL-33 restricts tumor growth and inhibits pulmonary metastasis in melanoma-bearing mice through eosinophils. Oncoimmunology 2017; 6: e1317420.
[25] Stevens RC, Cherezov V, Katritch V, Abagyan R, Kuhn P, Rosen H and Wüthrich K. The GPCR Network: a large-scale collaboration to determine human GPCR structure and function. Nat Rev Drug Discov 2013; 12: 25-34.
[26] Vivier E, Raulet DH, Moretta A, Caligiuri MA, Zitvogel L, Lanier LL, Yokoyama WM and Ugolini S. Innate or adaptive immunity? The example of natural killer cells. Science 2011; 331: 44-49.
[27] Salmon H, Idoyaga J, Rahman A, Leboeuf M, Remark R, Jordan S, Casanova-Acebes M, Khudoynazarova M, Agudo J, Tung N, Chakarov S, Rivera C, Hogstad B, Bosenberg M, Hashimoto D, Gnjatic S, Bhardwaj N, Palucka AK, Brown BD, Brody J, Ginhoux F and Merad M. Expansion and activation of CD103(+) dendritic cell progenitors at the tumor site enhances tumor responses to therapeutic PD-L1 and BRAF inhibition. Immunity 2016; 44: 924-938.
[28] Tran GT, Hodgkinson SJ, Carter NM, Verma ND, Plain KM, Boyd R, Robinson CM, Nomura M, Killingsworth M and Hall BM. IL-5 promotes induction of antigen-specific CD4+CD25+ T regulatory cells that suppress autoimmunity. Blood 2012; 119: 4441-4450.
[29] Taylor S, Huang Y, Mallett G, Stathopoulou C, Felizardo TC, Sun MA, Martin EL, Zhu N, Woodward EL, Elias MS, Scott J, Reynolds NJ, Paul WE, Fowler DH and Amarnath S. PD-1 regulates KLRG1(+) group 2 innate lymphoid cells. J Exp Med 2017; 214: 1663-1678.
[30] Zhang J, Qiu J, Zhou W, Cao J, Hu X, Mi W, Su B, He B, Qiu J and Shen L. Neuropilin-1 mediates lung tissue-specific control of ILC2 function in type 2 immunity. Nat Immunol 2022; 23: 237-250.

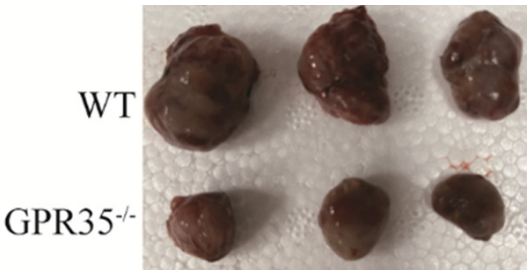


**Supplementary Figure 1.** The images of the tumors in the mice of the WT group and GPR35$^{-/-}$ group.

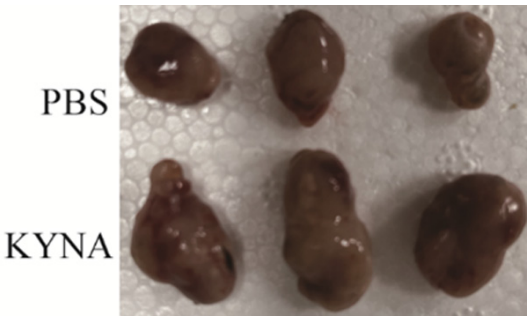


**Supplementary Figure 2.** The images of the tumors in the mice of the PBS group and KYNA group.

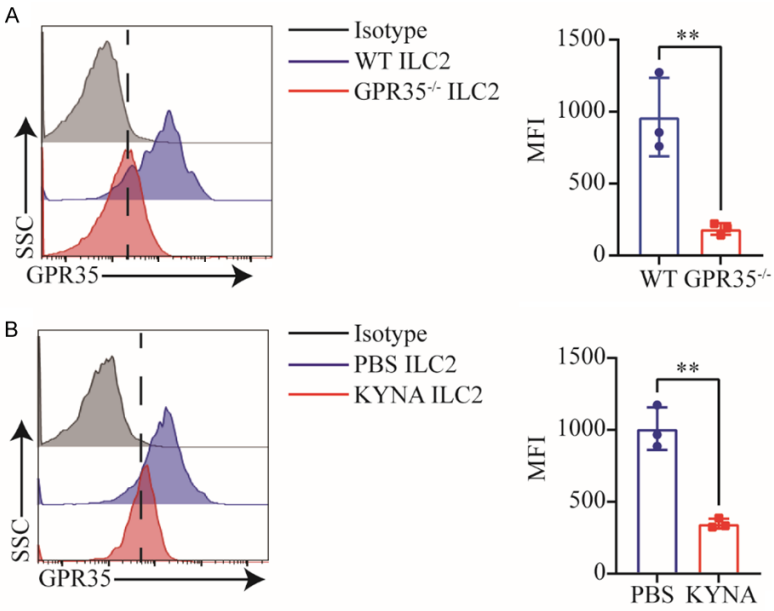


**Supplementary Figure 3.** The expression of GPR35 in GPR35$^{-/-}$ mice (A) and in KYNA treated Rag2$^{-/-}$ mice (B).

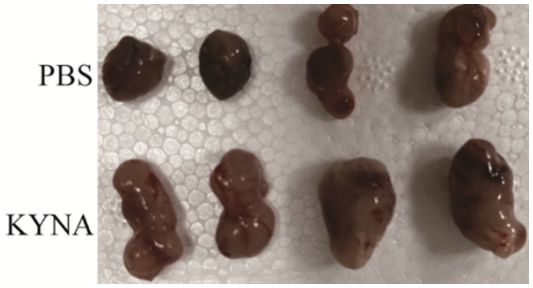


**Supplementary Figure 4.** The images of the tumors in the mice of the PBS group and KYNA group in Rag2$^{-/-}$ mouse.

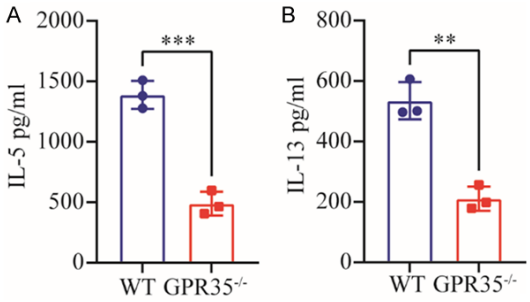


**Supplementary Figure 5.** The amount of IL-5 (A) and IL-13 (B) secreted by ILC2 from WT and GPR35$^{-/-}$ mice.

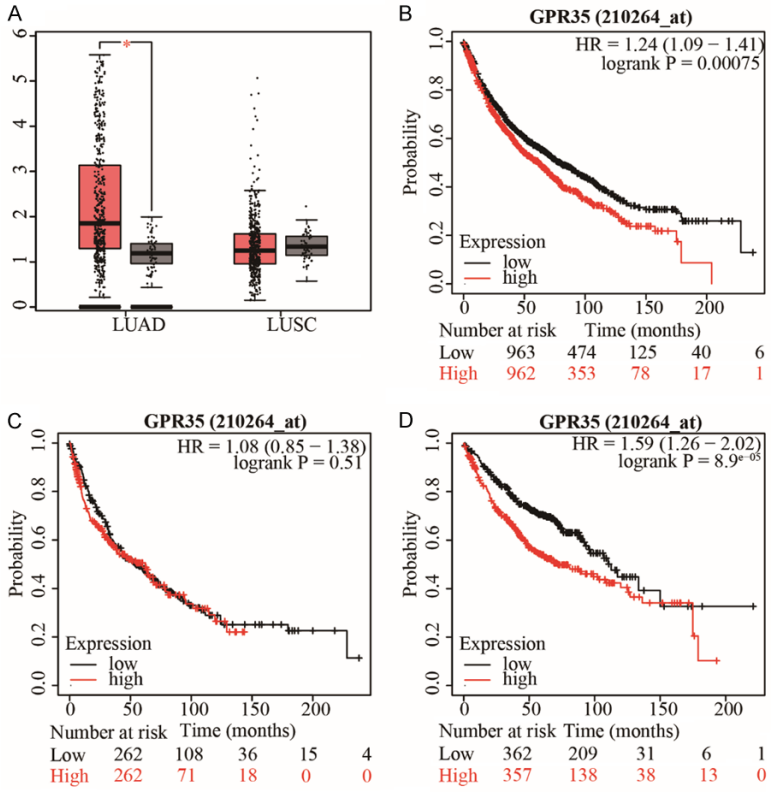


**Supplementary Figure 6.** GPR35 is a poor prognostic factor in lung adenocarcinoma. (A) The expression levels of GPR35 were elevated in the cancer tissues compared with normal tissues in LUAD. Lower GPR35 expression showed a better OS (B) and PFS (D). No prognostic significance was found based on squamous cell lung carcinoma (LUSC) (C). All experiments were carried out in triplicate; data are presented as mean SD. ***$P$ < 0.001, **$P$ < 0.01, *$P$ < 0.05, ns, no significant.